Title
CeO2 nanoparticles attenuate airway mucus secretion induced by TiO2 nanoparticles

Authors
Tsai, Shih-Ming
Duran-Robles, Edith
Goshia, Tyler
et al.

Publication Date
2018-08-01

DOI
10.1016/j.scitotenv.2018.03.001

Peer reviewed

HHS Public Access

Author manuscript

Sci Total Environ. Author manuscript; available in PMC 2019 August 01.

Published in final edited form as:

Sci Total Environ. 2018 August 01; 631-632: 262–269. doi:10.1016/j.scitotenv.2018.03.001.

CeO_2 nanoparticles attenuate airway mucus secretion induced by TiO_2 nanoparticles

Shih-Ming Tsai[1,†], **Edith Duran-Robles**[1,†], **Tyler Goshia**[1], **Maria Mesina**[1], **Carlos Garcia**[1], **Julia Young**[1], **Angelo Sibal**[1], **Meng-Hsuen Chiu**[1], and **Wei-Chun Chin**[1,*]

[1]Bioengineering Program, School of Engineering, University of California at Merced, Merced, CA 95343, USA

Abstract

Nanotoxicity studies associated with various nanoparticles (NPs) have attracted intense research interest due to the broader applications of nanoparticles in our daily lives. The exposure of nanoparticles can lead to hypersecretion and accumulation of airway mucus which are closely associated with many respiratory diseases. Titanium dioxide (TiO_2), one of the PM10 components, is a major NP that is widely utilized in many commercial products. Our previous study established the connection between induced airway mucus secretion and TiO_2 NPs. However, the countermeasure to reduce the harmful effects of TiO_2 NPs, especially airway mucus secretion, remains unexplored. One of the potential candidates to reduce airway mucus secretion is Cerium Oxide (CeO_2) NPs. It has been reported that CeO_2 NPs can protect cells by diminishing ROS and inflammatory responses. Herein, our study shows that CeO_2 NPs are able to reduce cytosolic Ca^{2+} changes and mitochondrial damage caused by TiO_2 NPs. Our results provide the evidence that hypersecretion of mucus and apoptosis progression induced by TiO_2 NPs can be attenuated by CeO_2 NPs. This study highlights the potential capacity of CeO_2 NPs as a supplementary material for TiO_2 NPs applications in the future.

Graphical Abstract

*Corresponding author: Wei-Chun Chin, Bioengineering Program, School of Engineering, University of California at Merced, Merced, CA 95343, USA, 5200 North Lake RD, Merced, CA 95343, USA, Tel: +1 209 228 8668, Fax: +1 209 228 4047, wchin2@ucmerced.edu.

†These authors contributed equally

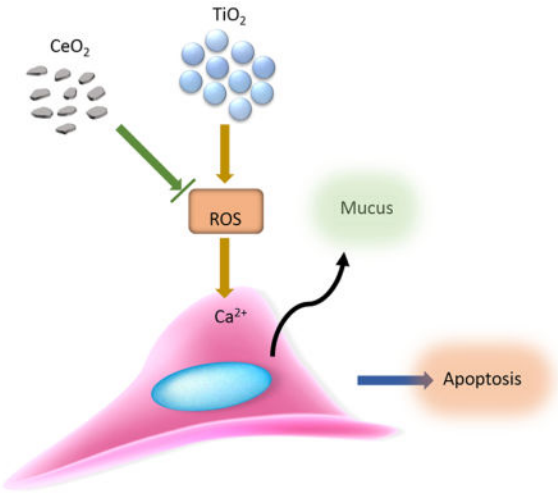

Keywords

Nanoparticles; BEAS-2B cell; Ca^{2+} signaling

1. Introduction

Nanoparticle (NP) exposure has been reported to increase pulmonary morbidity and mortality associated with respiratory diseases such as asthma, chronic obstructive pulmonary disease and Cystic Fibrosis (CF) (Alfaro-Moreno et al., 2007; Atkinson et al., 2001; Gwinn and Vallyathan, 2006; Ling and van Eeden, 2009; Sethi, 2004; Stone, 2000). Titanium oxide (TiO_2) is a common nanomaterial used in nanotechnology and pharmaceutical industries, and is also a main component in many household items (Shi et al., 2013). It has been shown to induce allergen-independent histamine release, causing mucus secretion and abnormal inflammatory responses (Chen et al., 2011; Chen et al., 2012). In addition to inhalation through the airways, these nanoparticles can also enter the human body by direct penetration, ingestion, and injection (Shi et al., 2013). The increased mucus secretion is directly correlated with the production of reactive oxygen species (ROS), and if chronic, may lead to the overproduction of ROS and radical formation. It has been reported that excessive cellular ROS can lead to the damage of lipids, proteins and nucleic acids that impair regular functional integrity of the cell and oxidative stress can also simulate apoptosis progression (Martin and Leibovich, 2005; Ray et al., 2012).

Cerium oxide (CeO_2) is a rare metal oxide catalyst that can be used for both industrial and biomedical applications, such as disel exhaust catalysis, oxygen sensors, as well as potentially providing protection against radialtion damage, oxidative stress, and inflammation (Asati et al., 2009; Younis et al., 2016). Its properties arise from Ceria's varying valence electrons that are either +3 or +4, and its large surface-area-to-volume ratio creates oxygen defects (Heckert et al., 2008; Korsvik et al., 2007). Earlier studies have suggested ceria can produce Reactive Oxygen Species (ROS) (De Marzi et al., 2013; Eom and Choi, 2009a; Lin et al., 2006; Park et al., 2008a) that can cause an immunological response in rats that included alveolar functional change, significant lung inflammation and

evident cytotoxicity (Eom and Choi, 2009a). Few studies on CeO_2 induced alveolar functional changes have indicated that additionally, CeO_2 may initiate and progress pulmonary fibrosis (Ma et al., 2012; Ma et al., 2011).

However, recent research has shown the ability of Ceria oxide to protect cells from death in certain concentrations (Dowding et al., 2014). Nitric Oxide (NO) combines with superoxide anions to form peroxynitrite anions which are highly reactive and toxic to the cell. Cerium oxide can act as radical scavengers as the enzyme superoxide dismutase to remove radicals formed during the overproduction of NO (Dowding et al., 2012). More interestingly, cerium oxide particle size (either at a micro or nano scale) did not appear to have a significant impact on its ability to scavenge ROS in human monocytic cell line U937 (Lord et al., 2012). Cerium oxide's unique properties may even expand toward nanoparticle therapy (Hirst et al., 2009).

In this study, we investigated the capability of Ceria NPs to reduce the toxicity effect from TiO_2 NP exposure in BEAS-2B epithelial cells by determining the ROS generation and mucus secretion response. We evaluated the changes of cytosolic Ca^{2+} ($[Ca^{2+}]_c$) by using direct NP stimulation to cells by fluorescent microscope. Furthermore, we also examined the differences in apoptosis progression with and without CeO_2 NPs present by using Caspase-3 and Cytochrome C assays.

2. Materials and Methods

2.1. Culture of Cells

The BEAS-2B epithelial cells were derived from normal bronchial epithelium obtained from autopsies of non-cancerous individuals. BEAS-2B is a commonly used cell model that screens for both chemical and biological agents, inducing and affecting differentiation, as well as carcinogenesis (Garcia-Canton et al., 2013; Sharma et al., 1994). Cells were grown and maintained in Dulbecco's Minimal Essential Medium (DMEM)/F12 supplemented with L-glutamine (5 mM), 1% Penicillin/Streptomycin, and 10% Fetal Bovine Serum (FBS). The BEAS-2B cells were cultured in 15-cm Falcon plates and incubated in a humidified incubator at 37°C, 5% CO_2. Cell counts were performed using trypan blue (Sigma) exclusion and a Bright-Line Hemocytometer. Cells were passed every 5 days or when confluence reached 80%.

2.2. Cell Preparation

Cells were seeded at 1×10^5 cells per well in a 96-well plate (75% confluence) for cell viability assays, 1×10^6 cells per well in a 4-well plate (75% confluence) for Ca^{2+} signaling, ROS and Mitochondria analysis. After seeding, cells were incubated for 24 hours in DMEM/F12 medium supplemented with 10% FBS. Following 24 hours of incubation, the medium was removed from the cells and the culture was rinsed with phosphate buffered saline twice (PBS). PBS wash was replaced with nanoparticles sonicated in Ca^{2+} containing Hanks or Ca^{2+}-Free Hanks.

2.3. Cell Viability Assay

Photocolorimetric determination of cytotoxicity was assessed using CCK-8 dye (Dojindo Laboratories, Tokyo, Japan)(Chen et al., 2008; Tsai et al., 2017). CCK-8, being non-radioactive, offers a colorimetric determination of the percentage of viable cells subjected to varying NP concentrations. This assay kit measures the metabolic activity of dehydrogenases within the viable cells to convert WST-8 Tetrazolium salt into water-soluble formazan. It was prepared by adding CCK-8 in HBSS in a 1:10 dilution. Cells were rinsed with HBSS and 100 μL of the dye was loaded into each well. Then, the cells were incubated in a 37°C, 5% CO_2 incubator for 6 h. The absorbance was measured by using a Thermo Multiscan EX plate reader (Thermo Multiskan EX plate reader, VWR, CA, USA) at the optical density of 450 nm (650 nm reference). An average was calculated from three separate data sets for each concentration, including the untreated control, from three independent experiments and was tabulated as a percentage of the untreated control.

The cell viability was calculated by $\frac{OD_{450treatment} - OD_{650treatment}}{OD_{450contorl} - OD_{650contorl}} * 100\,\%$.

2.4. CeO_2 Nanoparticle and TiO_2 Nanoparticle

A mixture of anatase and rutile forms of ultrafine titanium (IV) dioxide (<100 nm) (Sigma-Aldrich, MO, USA) was used in this study because this form has been shown to result in more severe cellular injuries (Chen et al., 2012; Gurr et al., 2005; Shi et al., 2013). The TiO_2 NPs have a surface area of 36 m^2/g and the dispersion conductivity is 1040 μS/cm (information from Sigma). Cerium oxide (CeO_2, 99.9%, 15–30 nm from Nanostructured & Amorphous Materials, Inc.) have a surface area of 30–50 m^2/g. All NP samples were sonicated before use. The concentrations used were 500 μg/ml, 250 μg/ml, 100 μg/ml, and 50 μg/ml. The range of concentrations used were consistent with the concentrations of TiO_2 and CeO_2 NPs found in previous reports (Chen et al., 2012; Dowding et al., 2014; Dowding et al., 2012; Gurr et al., 2005; Hirst et al., 2009; Niu et al., 2011). The TiO_2 and CeO_2 NPs were reconstituted with Hanks' solution (Invitrogen, CA, USA) before being tested individually and sonicated for approximately 5 minutes immediately before use.

2.5. Scanning Electron Microscope

TiO_2 and CeO_2 NPs were prepared into 5 μg/ml and drop casted on a clean silicon wafer and air dried to remove residual water. The size of NPs were independently confirmed using a Scanning Electron Microscope (Gemini SEM 500, Zeiss).

2.6. Intracellular Reactive Oxygen Species (ROS) Production

ROS production was evaluated by fluorescence microscopy using oxidation of CM-H2DCFDA dye (Invitrogen, CA, USA) (Chen et al., 2012). The cells (1×10^5 cells/well) were cultured for 24 hrs before being rinsed with PBS solution. Samples were stained by applying a loading buffer containing 2 μM reconstituted CM-H2DCFDA dye in medium for 30 minutes. The stained samples were washed with PBS three times and set aside for 5 minutes of recovery time for cellular esterases to hydrolyze the AM or acetate groups and render the dye responsive to oxidation. Hanks' buffer, containing TiO_2 NPs at concentrations

ranging from 0–500 μg/ml and CeO_2 NPs in 50 μg/ml, was then incubated with the cells for 15 minutes in 37°C followed by PBS washing. Fluorescent images of ROS generated in cells were captured and analyzed by calculating the ratio of increase in fluorescent intensity between different treatments and control groups.

2.7. Mitochondria Damage Measurement

The mitochondrial inner trans-membrane potential was assessed using polychromatic 5,5′, 6,6′-tetrachloro-1,1′,3,3′-tetraethylbenzimidoazolyl-carbocyanio iodide (JC-1 Sigma) (Tsai et al., 2017). JC-1 is a lipophilic fluorescent cation that can be incorporated into the mitochondrial membrane, where it is dependent on membrane potential state aggregates. Aggregation changes the fluorescence properties of JC-1, shifting from green to red fluorescence. Intact mitochondrial membranes stained with JC-1 exhibit a pronounced green mitochondrial fluorescence that is detectable by fluorescence microscopy. A breakdown of the mitochondrial membrane potential results in a subsequent decrease in green fluorescence and increase in red fluorescence. Prior to NPs stimulation, cells were washed with PBS twice and incubated with JC-1 staining reagent (1:1000) in medium at 37°C for 30 minutes, followed by washing with PBS and cell treatment. The mitochondrial membrane potential was detected by fluorescence microscopy at time intervals of 10 minutes.

2.8. Measurement of $[Ca^{2+}]_c$

All experiments were performed in dark conditions. The cells were loaded with a Rhod-2 AM dye (1 μM) (Kd = 570 nM, λ_{Ex} = 552 nm and λ_{Em} = 581 nm) (Invitrogen, CA, USA) for 45min. The cells were then washed with PBS twice before being incubated with Hanks buffer, and treated with the appropriate NPs concentration. All Ca^{2+} signaling experiments were carried out in a thermo-regulated state at 37°C mounted on a Nikon microscope (Nikon Eclipse TE2000- U, Tokyo, Japan) (Chen et al., 2008; Chen et al., 2011; Chen et al., 2012; Tsai et al., 2017).

2.9. Mucin Secretion and ELLA

The cells were seeded at 1×10^6 cells per well in a 6-well plate and cultured for 24 hours. BEAS-2B cells were then rinsed with PBS and stimulated for 15 minutes with the corresponding TiO_2 and CeO_2 NP concentrations (500 μg/ml, 250 μg/ml, and 100 μg/ml) prepared in PBS. The supernatant containing secreted mucin was collected and briefly centrifuged at 8,000 rpm to remove the residual NPs. The supernatant was then incubated in a 96 well (Nunc MaxiSorp, VWR, CA, USA) plate overnight at 4°C. Afterward the 96-well plate was washed with PBST (PBS + 0.05% Tween-20) and then blocked with 1% BSA. The 96 well plate was washed again with PBST and incubated with lectin (Wheat germ agglutinin, WGA) (Sigma-Aldrich, MO, USA), conjugated to horseradish peroxidase (HRP; 5 mg/ml) (Sigma-Aldrich, MO, USA), at 37°C for 1 hour. The substrate, 3,3′,5,5′-Tetramethylbenzidine (TMB; Sigma-Aldrich, MO, USA), was added to each well at room temperature, followed by H_2SO_4 (Sigma-Aldrich, MO, USA) in order to terminate the reaction. The optical density was measured at 450 nm (Chen et al., 2011; Kemp et al., 2004).

2.10. Immunosorbent Assay (ELISA) Preparation

The cells were seeded at a density of 1×10^6 cell density in a 6-well plate and cultured for 24 hours. BEAS-2B cells were then rinsed with PBS. Cells were stimulated for 2 hours with the appropriate TiO_2 and CeO_2 NPs concentrations (0–500 μg/ml) prepared in PBS. Cell lysing was prepared by the Peirce RIPA cell lysate reagent, and the lysate was collected and transferred to a microcentrifuge tube. The samples were centrifuged at ~14,000 × g for 15 minutes to pellet the cell debris and NPs. The supernatant was then incubated in a 96-well plate overnight at 4°C. Afterward the 96-well plate was washed with PBST (PBS + 0.05% Tween-20) and then blocked with 1% BSA. The 96 well plate was washed again with PBST and incubated with Rabbit Anti-Caspase 3, active form antibody (Millipore, polyclonal antibody) and Mouse anti-Cytochrome C (Invetrogen, monoclonal antibody) at room temperature for 2 hours. Then use secondary antibody (anti-rabbit and anti-mouse conjugated horseradish peroxidase, HRP, Millipore) and followed by the same procedure as ELLA to measure the absorbance intensity (Tsai et al., 2017).

2.11. Image Analysis

Image analysis was performed with an inverted Nikon Eclipse TE2000-U fluorescent microscope. Each photo was taken at 10x magnification and analyzed using Simple PCI (Compix Inc., Imaging Systems, Sewickle, PA, USA). The data shown for cytosolic calcium concentrations is represented by Rhod-2 Fluorescence. Images were taken every 0.5 second and automatically converted to grayscale for analysis. Simple PCI provided the pixel intensities (mean gray value) of selected areas, each with a mean fluorescence per frame for 200 cells over 100 s (~200 frames) immediately following nanoparticles stimulation. The data shown for immunofluorescence staining is a representation of protein expression after 1–2 hour treatments of graphene. All experiments were conducted and corroborated independently at least 3 times.

2.12. Statistical Analysis

The data was presented as mean ±SD. Each experiment was performed independently at least three times. Statistical significance was determined using a test analysis with p values < 0.05 (GraphPad Prism 4.0, GraphPad Software, Inc., San Diego, CA, USA).

3. Results and Discussion

3.1. NPs Characterization and Cell Viability Assay

Nanoparticle toxicity relies on the material's properties such as surface area, morphology, and size distribution. In order to characterize our material's properties prior to the toxicity study, we preferred to analyze the size distribution and surface structure by SEM. Both TiO_2 (Figure 1A) and CeO_2 NPs (Figure 1B) demonstrated a slight aggregation on the substrate surface, and these aggregations/NPs ranged from 1 μm to 10 μm in diameter respectively.

BEAS-2B cells have been selected for use in several different NPs toxicity studies (Eom and Choi, 2009a; Eom and Choi, 2009b; Gurr et al., 2005; Heng et al., 2010; Park et al., 2008a; Park et al., 2008b) and were adopted as our representative human bronchial epithelial cells. To evaluate the individual and collective in vitro toxicity data of TiO_2 and CeO_2 NPs, we

preformed the colorimetric CCK8 assay to determine cell viability results. The experimental conditions of TiO_2 NPs were consistent with our previous study (Chen et al., 2008; Chen et al., 2012). As shown in Figure 2A, there was no significant population change after 2 hours of treatment in the group treated with 50 μg/ml and 200 μg/ml CeO_2 NPs compared to the control group. However, there was a significant population survival rate increase in the group treated with 500 μg/ml TiO_2 NPs compared to the group co-treated with 50 μg/ml and 200 μg/ml CeO_2 NPs (Figure 2B).

3.2. Elimination of TiO_2 NPs Generated ROS by CeO_2 NPs

ROS is one of the major factors through which NPs cause nanotoxicity for the cell. Previous studies have shown that in lower concentrations of CeO_2 NPs, ROS can be scavenged to protect the cell (Dowding et al., 2012; Korsvik et al., 2007) due to the unique material properties of Cerium. From our results, we conclude that the 50 μg/ml CeO_2 NPs treated group has no significant difference from the control group. Our result shows (Figure 3) a decrease of around half the amount of generated ROS from co-treated cells with 500 μg/ml TiO_2 NPs and 50 μg/ml CeO_2 NPs compared to the TiO_2 NPs only group. The group with 250 μg/ml TiO_2 NPs treatment co-treated with CeO_2 50 μg/ml was still able to reduce around 100% of ROS production. The group treated with only CeO_2 NPs preformed the same as the control without any significant difference. The anti-ROS production ability of CeO_2 NPs can dramatically reduce the ROS production by TiO_2 NPs after 15 minutes of co-treatment, which is consistent with other reports (Niu et al., 2011).

3.3. $[Ca^{2+}]_c$ Change and Mucus Secretion (ELLA)

The Ca^{2+} channel on the cell membrane plays a critical role in cell signaling and response to changes in the environment. In our previous study, the $[Ca^{2+}]_c$ change highly influenced the airway cell response to the NP stimulation and determined the amount of mucus secretion. The resting $[Ca^{2+}]_c$ of BEAS-2B cells in HBSS fluctuated greatly with micro-environmental changes, and its regulation is one of the main determinants of fluid secretions in directly affecting the observed mucin secretions (Chen et al., 2010). Stimulation with TiO_2 NPs led to a rapid and transient increase in cytosolic calcium, whereas stimulation with CeO_2 NPs consistently remained minimal at different concentrations. The potential cytoprotective features of CeO_2 NPs were seen in cells that were co-stimulated with TiO_2 and CeO_2 NPs compared to cells treated with only TiO_2 NPs (Figure 3). The addition of 50 μg/ml CeO_2 NPs can reduce approximately 2/3 of fluorescent increase in 750 μg/ml TiO_2 group (Figure. 4A), and 3/4 of fluorescent increase in 500 μg/ml TiO_2 group (Figure. 4B). Furthermore, our result also demonstrated that CeO_2 NPs (50 μg/ml) have the capability to diminish the $[Ca^{2+}]_c$ increase caused by 250 μg/ml and 100 μg/ml of TiO_2 NPs (Figure. 4C, 4D).

Assessment of cell surface mucin secretions by ELLA (Enzyme-linked lectin assay) indicated significant differences between control and NP-stimulated cells, and significant dose-dependent differences between cells stimulated by both CeO_2 and TiO_2 NPs, as shown in Figure. 5. When compared to the control, co-treated (CeO_2 and TiO_2 NPs) stimulated cells increased mucin secretion by 25% (TiO_2 500 μg/ml + CeO_2 50 μg/ml), or 35% (TiO_2 500 μg/ml + CeO_2 200 μg/ml), which was significantly higher. Important to note are the significant dose-dependent differences between the combined NP treatments. Compared to

our positive control data of TiO_2 NPs 500 μg/ml alone (which had a 45% secretion increase), cells treated with both CeO_2 and TiO_2 NPs showed a reduction of 10–20% mucus secretion, indicating the potential of CeO_2 NPs in attenuating mucin secretion induced by TiO2 NPs.

3.4. Mitochondrial Damage and Apoptosis Processes Attenuated by CeO_2 NPs

Mitochondrial damage is the initial stage of apoptosis. ROS generation usually stimulates the downstream cellular response and fuels the apoptosis process. The results we observed were consistent with the trends of the ROS data, where the TiO_2 NPs only groups showed mitochondria damage after just 15 minutes of treatment with nanoparticles. The 500 μg/ml TiO_2 NP treatment had an increase of almost 100% mitochrondrial damage compared to the control group. The 250 μg/ml and 100 μg/ml TiO_2 NPs treatments resulted in similar amounts of mitochrondrial damage, which was around 50% more than the control. However, all samples with CeO_2 NPs co-treatments showed no significant differences compared to the untreated control group (Figure 6).

A significant dose-dependent change in Caspase-3 and Cytochrome C expression was observed after BEAS-2B cells were exposed to the CeO_2 and TiO_2 NPs. Caspase-3 results showed significant variation that suggest CeO_2 NPs could benefit the cell in low concentrations. Compared to TiO_2 NPs at 500 μg/ml which had an increased Caspase-3 expression ratio of 25% relative to the control. The co-treatment of CeO_2 and TiO_2 NPs illustrated significantly lower expression than TiO_2 NPs alone at 500 μg/ml (35% for 200 μg/ml CeO_2 NPs co-treatment and 30% for 50 μg/ml CeO_2 NPs co-treatment), which signifies the beneficial potential of CeO_2 NPs (Figure. 7A).

Cytochrome C results exhibited similar apoptotic behavior, where TiO_2 NPs at 500 μg/ml elicited a 25% increase in expression compared to the control group. The co-treatment of CeO_2 and TiO_2 NPs resulted in a significantly lower Cytochrome C expression than TiO_2 NPs alone at 500 μg/ml, whereas the co-treatment with 200 μg/ml and 50 μg/ml CeO_2 NPs expressed similar trends with the Caspase-3 results. Taken together, the Caspase-3 and Cytochrome C results strongly suggest that CeO_2 NPs can have an inhibitory effect on TiO_2 NPs induced apoptosis (Figure. 7B).

4. Conclusion

Recent nanotoxicity studies have attracted a lot of attention on the toxic effects of TiO_2 NPs due to their broad use in industrial and commercial products. TiO_2 NPs have two major crystal forms: Rutile and Anatase. TiO_2 NPs containing more crystals in anatase form have been reported to have higher cell toxicity (Shi et al., 2013). Thus, TiO_2 NPs are being considered as a kind of carcinogenic material due to the large amount of genereated ROS that will cause cell death and mutations. From our earlier studies, we demonstrated the possible mechanism of TiO_2 NPs toxicity on mast cells (Chen et al., 2012) and airway cells (Chen et al., 2010). Thus the exact mechanism of how CeO_2 NPs reduce the cytotoxicity of TiO_2 NPs requires further exploration. CeO_2 NPs are one of the new materials which interest many reserachers based on its similar material properties and lower potential toxicity. Several reports have provided important information about the toxic/anti-toxic properties of different sizes of CeO_2 NPs (Conway et al., 2014; Dowding et al., 2014; Eom and Choi,

2009a; Heckert et al., 2008; Hirst et al., 2009; Keller et al., 2014; Korsvik et al., 2007; Kumari et al., 2014; Niu et al., 2011; Park et al., 2008a). Although cytotoxicity level results have varied, we found that the short-term period treatment of CeO_2 NPs did not significantly affect cell viability. Our study shows the potential that CeO_2 NPs can reduce the ROS generated from TiO_2 NPs, which is consistent with previous studies (Heckert et al., 2008; Niu et al., 2011). However, by comparing our 50 μg/ml and 250 μg/ml of CeO_2 NPs treatments we can see that higher CeO_2 NPs concentration may affect cell viability due to the physical damage to the cell. Therefore, the optimal working concentration needs to be adjusted for further applications. Furthermore, we observed that the scavenging of ROS directly contributes to the $[Ca^{2+}]_c$ attenuation and less amount of mucus secretion. The result supports the notion that the presence of CeO_2 NPs can act as an anti-oxidase to attenuate hyperstimulation of foreign particle exposure for the BEAS-2B cell. CeO_2 can also reduce the initiation of apoptosis by protecting cells from mitochondria damages. Our study aimed to evaluate the co-effects of two different types of novel nanomaterials and established the capability of CeO_2 NPs reducing the effects of short term exposure by TiO_2 NPs. Our result suggests the possible application of CeO_2 NPs to reduce the health risks caused by commercial products containing TiO_2 NPs. However, further research must be done before CeO_2 can be incorporated as an active ingredient in commercial products.

Acknowledgments

This study was supported by grants from National Heart, Lung, and Blood Institute (1R15-HL-095039), National Science Foundation (CBET-0932404), and Linkou Chang Gung Memorial Hospital (CMRPG3F0601, CMRPD2F001 and CMRPG3D0082). The authors thank Xiao Tan for graphical abstract.

References

Alfaro-Moreno E, Nawrot TS, Nemmar A, Nemery B. Particulate matter in the environment: pulmonary and cardiovascular effects. Current opinion in pulmonary medicine. 2007; 13:98–106. [PubMed: 17255799]

Asati A, Santra S, Kaittanis C, Nath S, Perez JM. Oxidase-like activity of polymer-coated cerium oxide nanoparticles. Angewandte Chemie. 2009; 121:2344–2348.

Atkinson RW, Ross Anderson H, Sunyer J, Ayres J, Baccini M, Vonk JM, et al. Acute effects of particulate air pollution on respiratory admissions: results from APHEA 2 project. American journal of respiratory and critical care medicine. 2001; 164:1860–1866. [PubMed: 11734437]

Chen E, Ruvalcaba M, Araujo L, Chapman R, Chin W-C. Ultrafine titanium dioxide nanoparticles induce cell death in human bronchial epithelial cells. Journal of Experimental Nanoscience. 2008; 3:171–183.

Chen EY, Garnica M, Wang Y-C, Chen C-S, Chin W-C. Mucin secretion induced by titanium dioxide nanoparticles. PloS one. 2011; 6:e16198. [PubMed: 21283816]

Chen EY, Garnica M, Wang Y-C, Mintz AJ, Chen C-S, Chin W-C. A mixture of anatase and rutile TiO 2 nanoparticles induces histamine secretion in mast cells. Particle and fibre toxicology. 2012; 9:1. [PubMed: 22239852]

Chen EY, Wang Y-C, Chen C-S, Chin W-C. Functionalized positive nanoparticles reduce mucin swelling and dispersion. PloS one. 2010; 5:e15434. [PubMed: 21085670]

Conway JR, Hanna SK, Lenihan HS, Keller AA. Effects and implications of trophic transfer and accumulation of CeO2 nanoparticles in a marine mussel. Environmental science & technology. 2014; 48:1517–1524. [PubMed: 24410520]

De Marzi L, Monaco A, De Lapuente J, Ramos D, Borras M, Di Gioacchino M, et al. Cytotoxicity and genotoxicity of ceria nanoparticles on different cell lines in vitro. International journal of molecular sciences. 2013; 14:3065–3077. [PubMed: 23377016]

Dowding J, Song W, Bossy K, Karakoti A, Kumar A, Kim A, et al. Cerium oxide nanoparticles protect against Aβ-induced mitochondrial fragmentation and neuronal cell death. Cell Death & Differentiation. 2014; 21:1622–1632. [PubMed: 24902900]

Dowding JM, Dosani T, Kumar A, Seal S, Self WT. Cerium oxide nanoparticles scavenge nitric oxide radical (˙NO). Chemical communications. 2012; 48:4896–4898. [PubMed: 22498787]

Eom H-J, Choi J. Oxidative stress of CeO 2 nanoparticles via p38-Nrf-2 signaling pathway in human bronchial epithelial cell, Beas-2B. Toxicology letters. 2009a; 187:77–83. [PubMed: 19429248]

Eom H-J, Choi J. Oxidative stress of silica nanoparticles in human bronchial epithelial cell, Beas-2B. Toxicology in Vitro. 2009b; 23:1326–1332. [PubMed: 19602432]

Garcia-Canton C, Minet E, Anadon A, Meredith C. Metabolic characterization of cell systems used in in vitro toxicology testing: lung cell system BEAS-2B as a working example. Toxicol In Vitro. 2013; 27:1719–27. [PubMed: 23669205]

Gurr J-R, Wang AS, Chen C-H, Jan K-Y. Ultrafine titanium dioxide particles in the absence of photoactivation can induce oxidative damage to human bronchial epithelial cells. Toxicology. 2005; 213:66–73. [PubMed: 15970370]

Gwinn MR, Vallyathan V. Nanoparticles: health effects: pros and cons. Environmental health perspectives. 2006:1818–1825. [PubMed: 17185269]

Heckert EG, Karakoti AS, Seal S, Self WT. The role of cerium redox state in the SOD mimetic activity of nanoceria. Biomaterials. 2008; 29:2705–2709. [PubMed: 18395249]

Heng BC, Zhao X, Xiong S, Ng KW, Boey FY-C, Loo JS-C. Toxicity of zinc oxide (ZnO) nanoparticles on human bronchial epithelial cells (BEAS-2B) is accentuated by oxidative stress. Food and Chemical Toxicology. 2010; 48:1762–1766. [PubMed: 20412830]

Hirst SM, Karakoti AS, Tyler RD, Sriranganathan N, Seal S, Reilly CM. Anti-inflammatory Properties of Cerium Oxide Nanoparticles. Small. 2009; 5:2848–2856. [PubMed: 19802857]

Keller J, Wohlleben W, Ma-Hock L, Strauss V, Gröters S, Küttler K, et al. Time course of lung retention and toxicity of inhaled particles: short-term exposure to nano-Ceria. Archives of toxicology. 2014; 88:2033–2059. [PubMed: 25273020]

Kemp PA, Sugar RA, Jackson AD. Nucleotide-mediated mucin secretion from differentiated human bronchial epithelial cells. American journal of respiratory cell and molecular biology. 2004; 31:446–455. [PubMed: 15231488]

Korsvik C, Patil S, Seal S, Self WT. Superoxide dismutase mimetic properties exhibited by vacancy engineered ceria nanoparticles. Chemical Communications. 2007:1056–1058. [PubMed: 17325804]

Kumari M, Singh SP, Chinde S, Rahman MF, Mahboob M, Grover P. Toxicity study of cerium oxide nanoparticles in human neuroblastoma cells. International journal of toxicology. 2014 1091581814522305.

Lin W, Huang Y-w, Zhou X-D, Ma Y. Toxicity of cerium oxide nanoparticles in human lung cancer cells. International journal of toxicology. 2006; 25:451–457. [PubMed: 17132603]

Ling SH, van Eeden SF. Particulate matter air pollution exposure: role in the development and exacerbation of chronic obstructive pulmonary disease. Int J Chron Obstruct Pulmon Dis. 2009; 4:233–243. [PubMed: 19554194]

Lord MS, Jung M, Teoh WY, Gunawan C, Vassie JA, Amal R, et al. Cellular uptake and reactive oxygen species modulation of cerium oxide nanoparticles in human monocyte cell line U937. Biomaterials. 2012; 33:7915–7924. [PubMed: 22841920]

Ma JY, Mercer RR, Barger M, Schwegler-Berry D, Scabilloni J, Ma JK, et al. Induction of pulmonary fibrosis by cerium oxide nanoparticles. Toxicology and applied pharmacology. 2012; 262:255–264. [PubMed: 22613087]

Ma JY, Zhao H, Mercer RR, Barger M, Rao M, Meighan T, et al. Cerium oxide nanoparticle-induced pulmonary inflammation and alveolar macrophage functional change in rats. Nanotoxicology. 2011; 5:312–325. [PubMed: 20925443]

Martin P, Leibovich SJ. Inflammatory cells during wound repair: the good, the bad and the ugly. Trends in cell biology. 2005; 15:599–607. [PubMed: 16202600]

Niu J, Wang K, Kolattukudy PE. Cerium oxide nanoparticles inhibits oxidative stress and nuclear factor-κB activation in H9c2 cardiomyocytes exposed to cigarette smoke extract. Journal of Pharmacology and Experimental Therapeutics. 2011; 338:53–61. [PubMed: 21464334]

Park E-J, Choi J, Park Y-K, Park K. Oxidative stress induced by cerium oxide nanoparticles in cultured BEAS-2B cells. Toxicology. 2008a; 245:90–100. [PubMed: 18243471]

Park E-J, Yi J, Chung K-H, Ryu D-Y, Choi J, Park K. Oxidative stress and apoptosis induced by titanium dioxide nanoparticles in cultured BEAS-2B cells. Toxicology letters. 2008b; 180:222–229. [PubMed: 18662754]

Ray PD, Huang B-W, Tsuji Y. Reactive oxygen species (ROS) homeostasis and redox regulation in cellular signaling. Cellular signalling. 2012; 24:981–990. [PubMed: 22286106]

Sethi S. New developments in the pathogenesis of acute exacerbations of chronic obstructive pulmonary disease. Current opinion in infectious diseases. 2004; 17:113–119. [PubMed: 15021050]

Sharma S, Stutzman JD, Kelloff GJ, Steele VE. Screening of potential chemopreventive agents using biochemical markers of carcinogenesis. Cancer Res. 1994; 54:5848–55. [PubMed: 7954413]

Shi H, Magaye R, Castranova V, Zhao J. Titanium dioxide nanoparticles: a review of current toxicological data. Particle and fibre toxicology. 2013; 10:15. [PubMed: 23587290]

Stone V. Environmental air pollution. American journal of respiratory and critical care medicine. 2000; 162:S44–S47. [PubMed: 10934133]

Tsai S-M, Bangalore P, Chen EY, Lu D, Chiu M-H, Suh A, et al. Graphene-induced apoptosis in lung epithelial cells through EGFR. Journal of Nanoparticle Research. 2017; 19:262.

Younis, A., Chu, D., Li, S. Functionalized Nanomaterials. InTech; 2016. Cerium Oxide Nanostructures and their Applications.

HIGHLIGHTS

- CeO_2 NPs attenuate the toxicity effect caused by TiO_2 NPs.
- Cytosolic Ca^{2+} change and mucus secretion can be diminished by CeO_2 NPs.
- CeO_2 NPs inhibit BEAS-2B cell apoptosis progression.

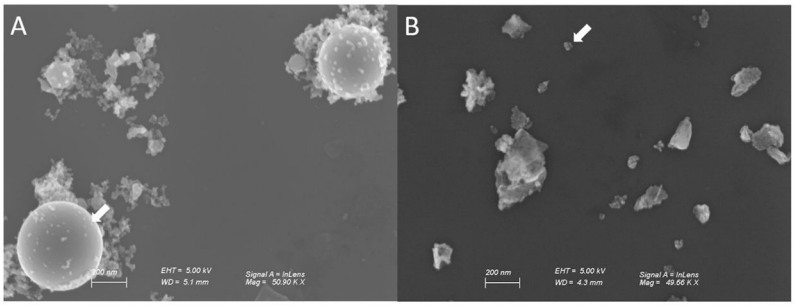

Figure 1.

SEM image of NP characteristics. The characterization of A) Single TiO_2 NPs (white arrow) and B) Single CeO_2 NPs (white arrow) on the substrate.

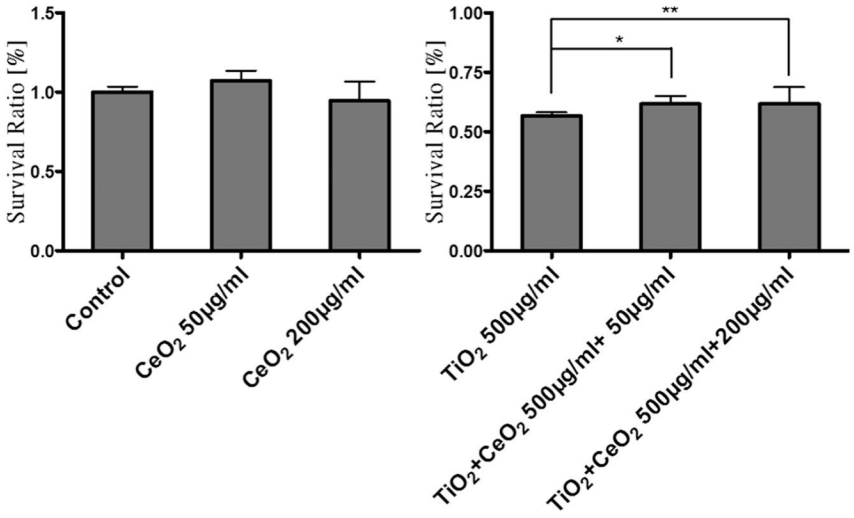

Figure 2.

Cell viability assay. A) There is no significant cell population change with different concentration of CeO_2 NPs treatment, B) but have significant population decrease after 2 hours of treatment in groups treated with different concentrations of TiO_2 and CeO_2 NPs. (*, **: n>6, P<0.05)

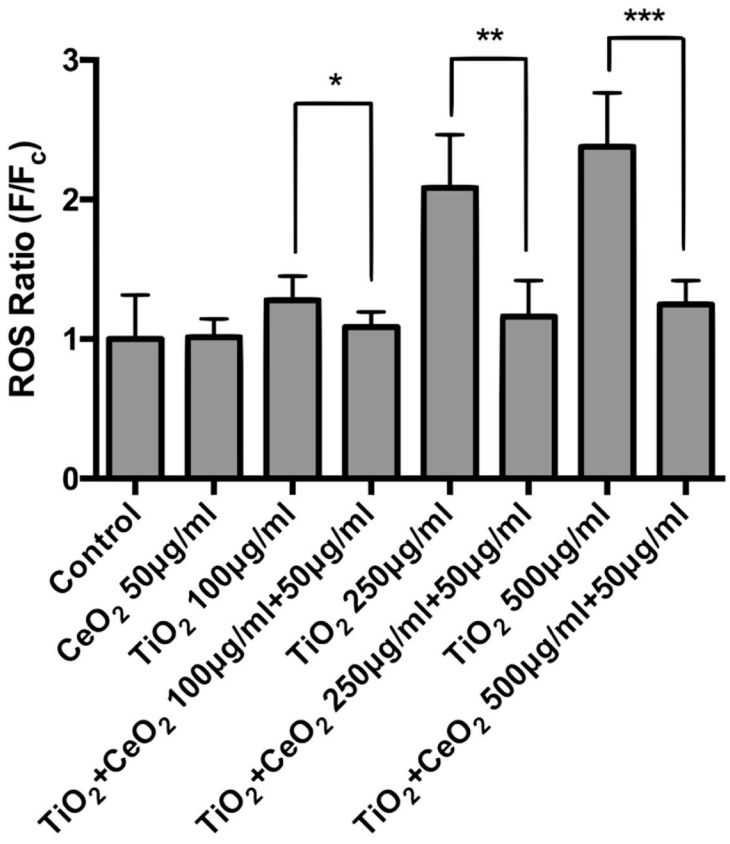

Figure 3.

ROS production. Fluorescent intensity results of ROS indicator dye in 8 different conditions of treatment on BEAS-2B cell (Combination of 50 μg/ml CeO_2 NPs and 100, 250, 500 μg/ml of TiO_2 NPs). (*, **, ***: n>100, P<0.05)

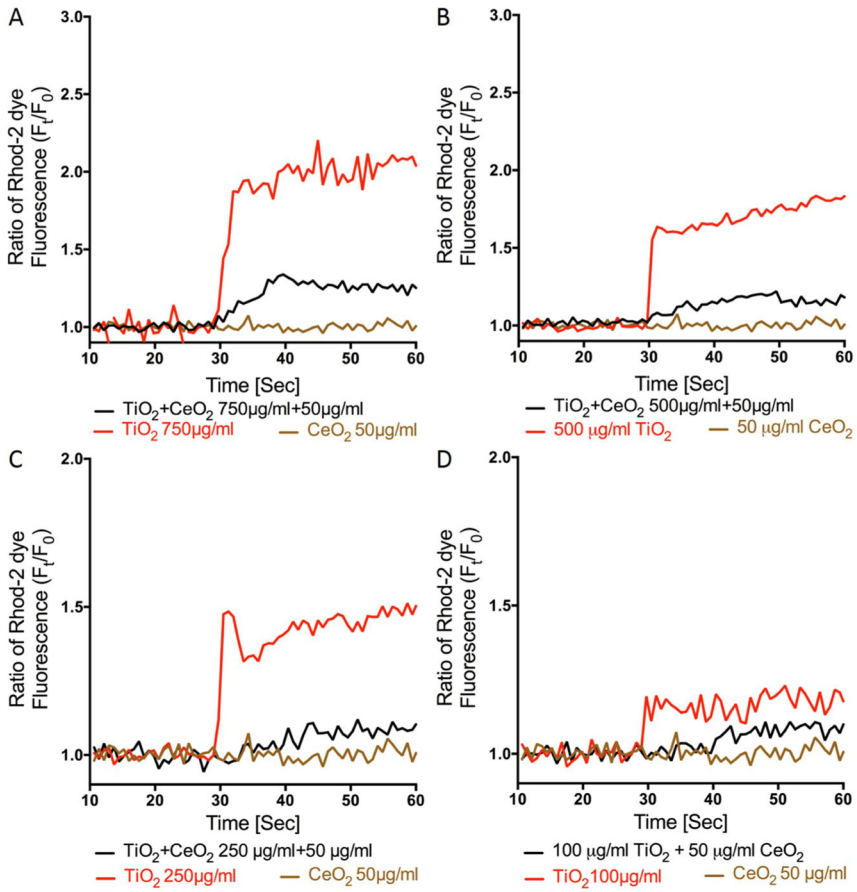

Figure 4.

Cytosolic Ca^{2+} change. $[Ca^{2+}]c$ change in BEAS-2B cells by in vitro TiO_2 NP delivery cotreated with CeO_2 NPs. Comparisons from A) 750 ug/ml, B) 500 ug/ml, C) 250 ug/ml, D) 100 ug/ml TiO_2 NPs. (Each line represents fluorescence intensity of 200 cells)

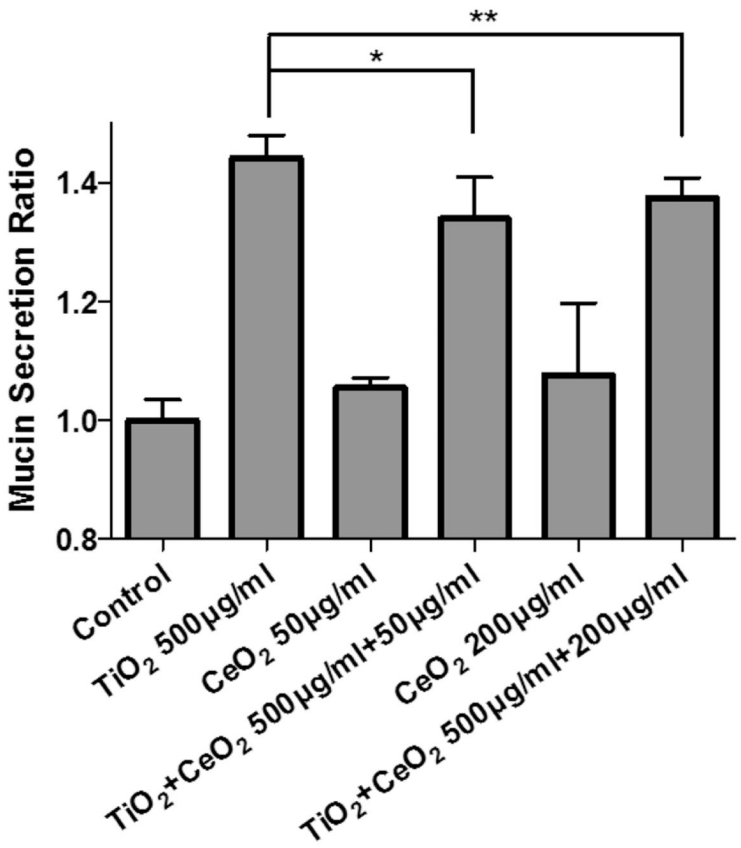

Figure 5.

Mucin secretion assay. Correlation analysis between the conjugate NP concentrations and mucin secretion of varying concentrations of 500 μg/ml TiO_2+50 μg/ml CeO_2, 500 μg/ml TiO_2+200 μg/ml CeO_2, 500 μg/ml TiO_2 using an ELLA assay. (*, **: n>6 P<0.05)

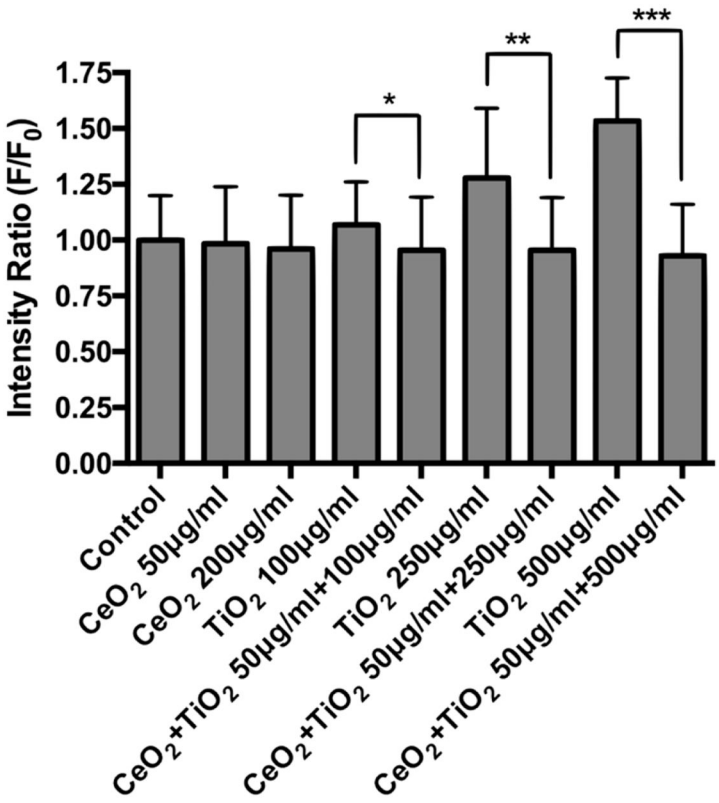

Figure 6.

Mitochondria damage assay. Fluorescent intensity results of JC-1 indicator dye in 9 different conditions of treatment on BEAS-2B cell (Combination of 50 μg/ml CeO_2 NPs and 100, 250, 500 μg/ml of TiO_2 NPs). (*, **, ***: n>100, P<0.05)

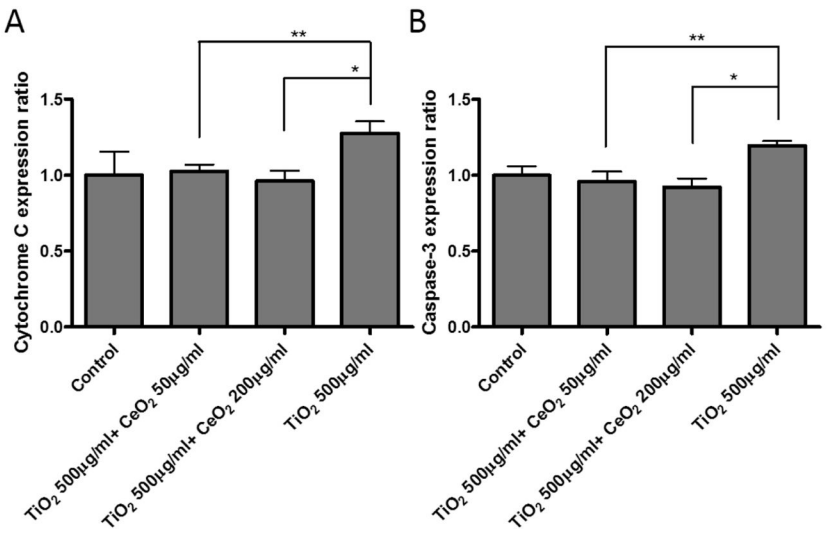

Figure 7.

Apoptosis marker ELISA results. Cells were treated with 500 μg/ml TiO_2 NPs only, or co-treated with 200 μg/ml and 50 μg/ml CeO_2 NPs, A) Cytochrome C and B) Caspase-3. (*, **: n>6, P<0.05)